

Sensitive 2,4-dinitrotoluene fluorescence sensors based on porous electrospun fibres and porous membranes

Pimpaka Putthithanad^a, Tidapa Rattanaumpa^a, Thidarat Pandhumas^b, Surangkha Budsombat^{a,b,*}

^a Department of Chemistry, Faculty of Science, Khon Kaen University, Khon Kaen 40002 Thailand

^b Materials Chemistry Research Centre,

Department of Chemistry and Centre of Excellence for Innovation in Chemistry, Faculty of Science, Khon Kaen University, Khon Kaen 40002 Thailand

^{a,b} Institute of Nanomaterials Research and Innovation for energy (IN-RIE), Research Network of NANOTEC-KKU (RNN), Khon Kaen University, Khon Kaen 40002 Thailand

*Corresponding author, e-mail: surama@kku.ac.th

Received 21 Feb 2018

Accepted 28 Feb 2019

ABSTRACT: Simple approaches for developing sensitive fluorescence sensors for 2,4-dinitrotoluene (DNT) detection were reported. Pyrene-doped poly(methyl methacrylate) (PMMA) and poly(vinyl chloride-co-vinyl acetate-co-vinyl alcohol) (PVC terpolymer) fibres, polystyrene (PS) fibres, and poly(styrene-co-methyl methacrylate) (PS-co-PMMA) fibres were prepared via electrospinning technique. Fibre morphology was studied using scanning electron microscopy. Sensing performance towards DNT was monitored through fluorescence emission of pyrene. The time dependence of quenching was observed for all fibres. Polymer matrix was found to affect DNT sensing, where PS fibres and PS-co-PMMA fibres showed slightly higher quenching efficiencies than PMMA-PVC terpolymer fibres. Enhanced quenching efficiency was achieved through introduction of porosity using poly(ethylene glycol)-400 (PEG) as a porogen to PMMA-PVC terpolymer fibres. The effect of porosity on sensing performance was further explored in pyrene-doped PS-co-PMMA membrane. Porous membrane prepared from a solution with PS-co-PMMA to PEG ratio of 1:1 provided higher sensing performance towards DNT than dense PS-co-PMMA membrane, possibly resulting from the increased surface area.

KEYWORDS: electrospinning, explosive, porogen, pyrene, quenching

INTRODUCTION

Due to concerns in anti-terrorism and homeland security, the development of sensors for detection of nitroaromatic explosives, which are the primary military explosives, is of great interest. The detection of explosives in vapour phase is challenging since the vapour pressure is extremely low. Among current detection methods, fluorescence method has attracted much attention due to short response time, high sensitivity, and simplicity.

Poly(acrylic acid)-poly(pyrene methanol) fibres were reported to detect 2,4-dinitrotoluene (DNT) effectively¹. The use of pyrene as a fluorescent indicator provided large Stokes shift, high quantum yield, strong absorbance, and excellent photostability and lifetime. A very high quenching efficiency of 81% towards 2,4,6-trinitrotoluene (TNT) after 9 min of exposure time was observed for flexible nanonets from pyrene, poly(vinylpyrrolidone) (PVP), 3-aminopropyl triethoxysilane (APTS), and

reduced graphene oxide (rGO)². Furthermore, these nanonets showed high selectivity towards TNT and DNT vapours. Wang et al reported that pyrene-doped polystyrene (PS) electrospun fibres exhibited higher sensitivity towards DNT compared to fibres prepared from polyethylene oxide, polyacrylonitrile, and PVP. The sandwich-like conformation between pyrene and phenyl pendants of PS was expected to provide a long-range exciton migration, leading to amplified fluorescence quenching³.

High surface area-to-volume ratio materials have been shown to provide higher sensitivity over thin membranes. Yang et al reported that upon introduction of secondary porous structures into nanofibres of tetrakis(4-methoxyphenyl)porphyrin and PS using Triton X-100 as a porogen, the sensitivity of the fibres towards DNT solution was enhanced approximately 5 times⁴. This group also prepared fluorescent porous cellulose acetate nanofibres by either introducing a porogen (Triton X-100 or PEG-4000) or deacetylation treatment,

and tested the fibres towards methyl violet⁵. The improvement in fluorescence quenching sensitivity with secondary porous structures was observed, and this could be attributed to the increased surface area, which facilitated quenchers to diffuse into nanofibres. In addition, our group recently reported the enhancement in Fe³⁺ detection using pyrene as a chromophore through the introduction of polystyrene and porous structures⁶. In this work, pyrene-doped fibres from three different polymer solutions, that is, poly(methyl methacrylate) (PMMA) and poly(vinyl chloride-co-vinyl acetate-co-vinyl alcohol) (PVC terpolymer), polystyrene (PS), and poly(styrene-co-methyl methacrylate) (PS-co-PMMA), were prepared via electrospinning technique. Sensing performances of these fibres towards DNT were studied and compared to that of solution-cast membrane. Furthermore, in order to increase the surface area, porous fibres and porous membranes were prepared using poly(ethylene glycol)-400 (PEG) as a water-soluble porogen. PEG removal was confirmed by attenuated total reflection Fourier transform infrared spectroscopy (ATR-FTIR) and scanning electron microscopy (SEM). The effect of porosity on DNT detection was discussed.

MATERIALS AND METHODS

Materials

Polystyrene (PS, average M_w 100 000 g/mol), poly(styrene-co-methyl methacrylate) (PS-co-PMMA, average M_w 100 000–150 000, 40 mol% styrene), poly(methyl methacrylate) (PMMA, average MW 120,000), poly(vinyl chloride-co-vinyl acetate-co-vinyl alcohol) (PVC terpolymer, PVC:PVAc:PVA = 90:4:6, average M_n 20 000), pyrene (98%), and 2,4-dinitrotoluene (97%) were purchased from Sigma-Aldrich (US). Poly(ethylene glycol) (PEG, M_n 400), *N,N*-dimethylformamide (DMF), and tetrahydrofuran (THF) were obtained from Fluka Chemical (US). All chemicals were used as received.

Fibre preparation by electrospinning

Pyrene-doped PS fibres and PS-co-PMMA fibres were prepared by dissolving polymer in DMF (30 wt.%), and pyrene (20% by weight of polymer) was added. The solution was stirred until forming homogeneous solution. The polymer solution was transferred into a plastic syringe equipped with 22-gauge stainless steel needle and was connected to a high voltage power supply. The voltage applied was 20 kV. The working distance between the syringe tip and

aluminium foil on collector was 15 cm. The electrospun solution was fed at a flow rate 1 ml/h. All experiments were performed at room temperature. Pyrene-doped electrospun PMMA-PVC terpolymer fibres and porous PMMA-PVC terpolymer fibres from 30% PEG solution were prepared as previously reported⁷.

Membrane preparation

A 5 wt.% PS-co-PMMA solution was prepared by dissolving PS-co-PMMA and pyrene (20% by weight of PS-co-PMMA) in THF. The solution was stirred for 24 h prior to casting on a Petri dish. The membrane was dried at room temperature, and later peeled off. PS membrane was prepared in the same manner. In a preparation of porous membrane, PEG was added to PS-co-PMMA/pyrene solution prior to stirring for 24 h. The weight ratios of PS-co-PMMA to PEG were 1:1 and 2:1. The solution-cast membrane was dried at room temperature, and later peeled off. As PEG is water-soluble, it was consequently washed away from the membrane by immersing in deionized water with a shaking speed of 120 rpm.

Characterization

Surface morphology was studied using a scanning electron microscope (SEM, SEC Co., Ltd., SNE-4500M). The average diameters of fibres were determined from 200 measurements in each micrograph using WCIF ImageJ. Attenuated total reflection Fourier transform infrared (ATR-FTIR) spectra were measured on a Bruker FTIR spectrometer (Tensor 27) with Opus 7.0 software measuring in the range of 4000–600 cm⁻¹. Emission spectra were recorded using an RF-5301PC spectrofluorophotometer (Shimadzu).

Response performance towards DNT

Sensing performances of pyrene-doped fibres and membranes towards DNT were carried out as follows. The sample was cut into 1 × 1 cm² piece. DNT (0.3 mg) was loaded in an aluminium container and placed in the cuvette with cover for 24 h to reach a saturation vapour pressure. To ensure that fluorescence emission was taken at the exact same spot, the sample was placed in the cuvette, and fluorescence emission was measured after 2 min. The excitation wavelength was 336 nm, and emission data was collected in the wavelength region of 350–650 nm. The maximum emission at 465 nm was recorded and used as initial emission F_i . The fluorescence emission (F) was then measured every certain time

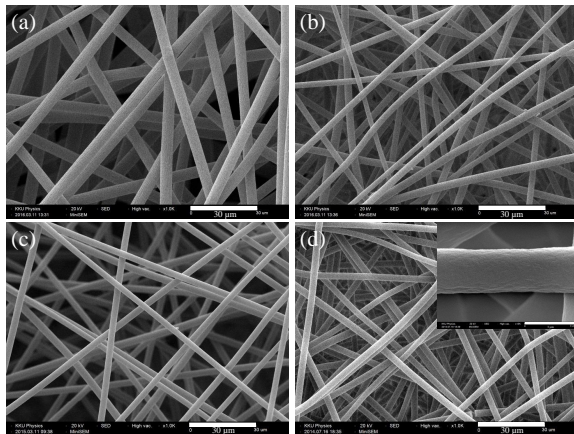


Fig. 1 SEM images ($\times 1k$, scale bar = 30 μm) of (a) pyrene-doped PS fibres, (b) PS-co-PMMA fibres, (c) PMMA-PVC terpolymer fibres, and (d) porous PMMA-PVC terpolymer fibres. The inset shows higher magnification ($\times 15k$, scale bar = 3 μm).

over 35 min. The fluorescence quenching efficiency was calculated from the equation: $1 - F/F_i$, where F_i and F are initial fluorescence intensity and fluorescence intensity at a certain time, respectively. The reported quenching efficiency was the mean of two replicates.

RESULTS AND DISCUSSION

Fibre preparation and fibre morphology

Solution properties play important roles in fibre formation via electrospinning. The critical chain overlap concentration (c^*) was calculated from $c^* = 1/[\eta]$, and the intrinsic viscosity was obtained from Mark-Houwink-Sakurada equation⁸, $[\eta] = KM^a$, where M is molecular weight of a linear polymer, K and a are Mark-Houwink parameters, which depend on the polymer, solvent and temperature. Eda et al⁹ reported that smooth fibres were obtained from 37.5 wt.% PS solution in DMF ($K = 0.0318 \text{ cm}^3/\text{g}$, $a = 0.603$) with c/c^* value of 13.8. In this work, the c^* value of 100k PS solution in DMF (30 wt.%) was 2.9 wt.%, and the c/c^* value was 10.3. This concentration provided smooth fibres without bead (Fig. 1). PS-co-PMMA fibres were prepared in the same manner. Even though observable PS-co-PMMA fibre mat was rather fluffy, uniform and bead-free fibres were obtained. The thicknesses of the three fibre mats were about 0.4 mm. PS fibres had the largest diameter, followed by PS-co-PMMA fibres, and PMMA-PVC terpolymer fibres, respectively (Table 1). Porous PMMA-PVC terpolymer/pyrene

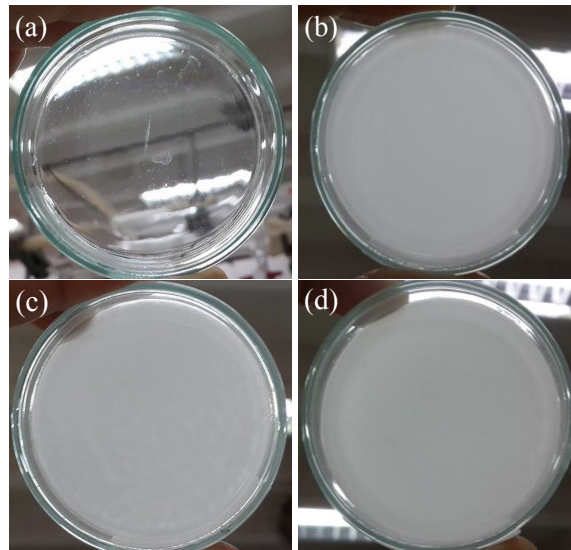


Fig. 2 SEM images (Photographs of as-prepared (a) pyrene-doped PS membrane and (b) PS-co-PMMA membrane; PS-co-PMMA/PEG membranes with PS-co-PMMA:PEG of (c) 1:1 and (d) 2:1.

fibres were prepared using 30% PEG. PEG was completely removed after 1 day of immersion in water as confirmed by FTIR and thermogravimetric analysis (data not shown)⁷. No significant changes in fibre thickness and fibre diameter were observed after PEG removal.

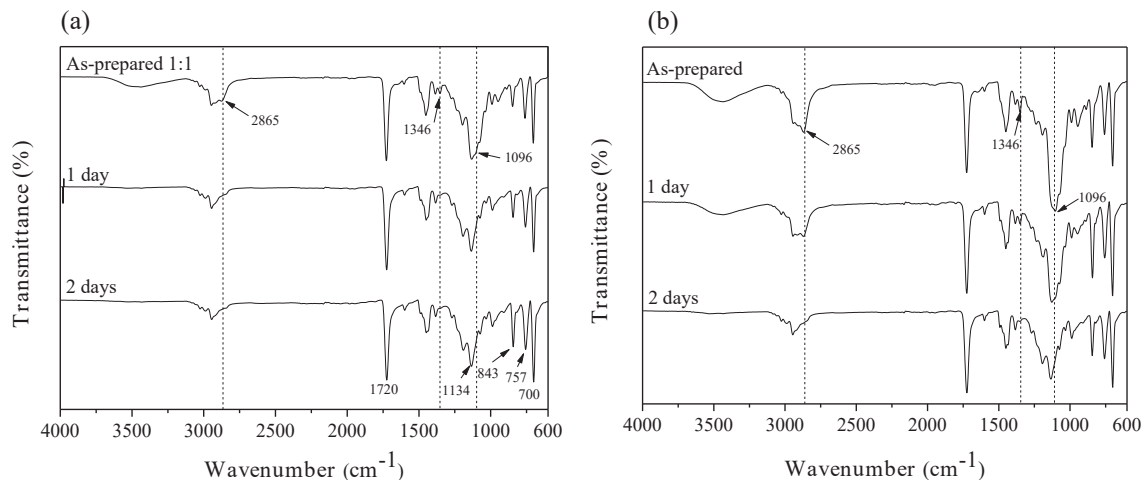
Membrane and porous membrane preparations

Homogeneous and self-standing pyrene-doped PS membrane, PS-co-PMMA membrane, and PS-co-PMMA/PEG membranes with thickness of about 0.24–0.25 mm were obtained (Fig. 2). PS membrane was brittle, while PS-co-PMMA membrane series were flexible. In a preparation of porous PS-co-PMMA membrane, PEG removal was confirmed using FTIR and SEM. FTIR spectra of the membrane with PS-co-PMMA to PEG ratio of 1:1 before and after immersion in water for 1 day and 2 days were shown in Fig. 3. Characteristic bands of PMMA at 1720 and 1134 cm^{-1} were designated to C=O stretching, and C–O stretching, respectively¹⁰. Absorption bands corresponding to aromatic ring of PS were shown at 757 and 700 cm^{-1} ¹¹. Characteristic band of pyrene at 843 cm^{-1} was assigned to C=C stretching, and bands at 749 and 700 cm^{-1} assigning to adjacent C–H stretching were overlapped with those of PS¹². Bands at 2865, 1346, and 1096 cm^{-1} of PEG were related to C–H stretching, C–H bending, and C–O stretching, respectively¹³. The

Table 1 Thickness of fibre mats and solution-cast membranes, fibre diameter, pore number, and pore size of PS-co-PMMA/pyrene/PEG membranes after immersion in water for 2 days.

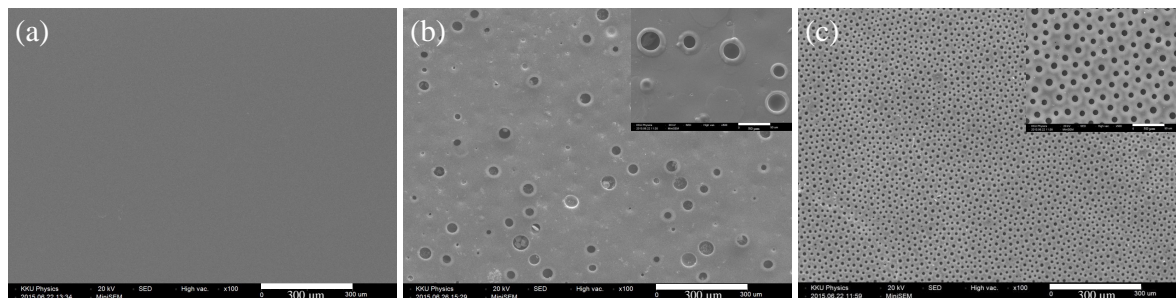
Matrix	Thickness (mm)	Fibre diameter (μm)	Pore number ^a	Pore size ^a (μm)
Fibre				
PS	0.39	5.39 ± 0.56	–	–
PS-co-PMMA	0.41	3.44 ± 0.60	–	–
PMMA-PVC terpolymer	0.37	2.79 ± 0.24	–	–
PMMA-PVC terpolymer:PEG = 1:0.3	0.38	2.95 ± 0.31	–	–
Membrane				
PS	0.24	–	–	–
PS-co-PMMA	0.25	–	–	–
PS-co-PMMA:PEG = 1:1	0.26	–	6	30.2 ± 9.4
PS-co-PMMA:PEG = 2:1	0.25	–	104	8.8 ± 1.4

^a Obtained from SEM images with the magnification of 500.

**Fig. 3** FTIR spectra of pyrene-doped PS-co-PMMA:PEG of (a) 1:1 membrane and (b) 2:1 membrane before and after immersion in water for 1 day and 2 days.

disappearance of bands corresponding to PEG at 2865, 1346, and 1096 cm^{-1} after 2 days of immersion suggested that PEG was completely removed.

The disappearance of these three bands was also observed for 2:1 membrane after 2 days of immersion in water (Fig. 3). SEM images of the prepared mem-

**Fig. 4** SEM images ($\times 100$, scale bar = 300 μm) of (a) pyrene-doped PS-co-PMMA membrane, (b) porous 1:1 membrane, and (c) porous 2:1 membrane. The inset shows higher magnification ($\times 500$, scale bar = 50 μm).

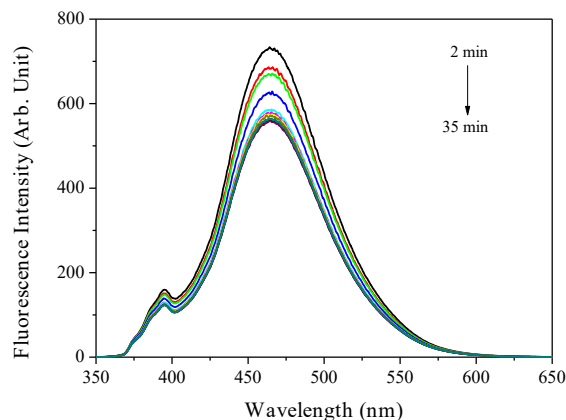


Fig. 5 Emission spectra of pyrene-doped PMMA-PVC terpolymer fibres as a function of exposure time to DNT vapour.

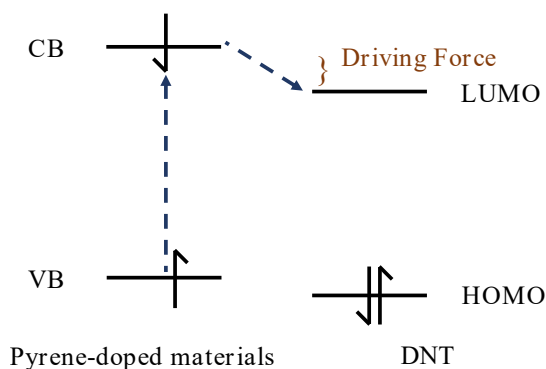


Fig. 6 Electron transfer mechanism for pyrene-doped materials by DNT.

branes were shown in Fig. 4. The surface of PS-co-PMMA membrane was smooth, while porous structures were observed for PEG-containing membranes after immersion in water for 2 days. The average pore sizes were reported in Table 1. The pore size of the membranes increased with increasing PEG content. Relatively ordered porous structures were shown in 2:1 membrane.

Sensing performance towards DNT

Fibres

Emission spectra of pyrene-doped PMMA-PVC terpolymer fibres were shown as representative in Fig. 5. The emission spectra showed two major bands. The first weak band between 370 and 420 nm could be ascribed to the emission from excited pyrene monomer¹⁴. The second strong band

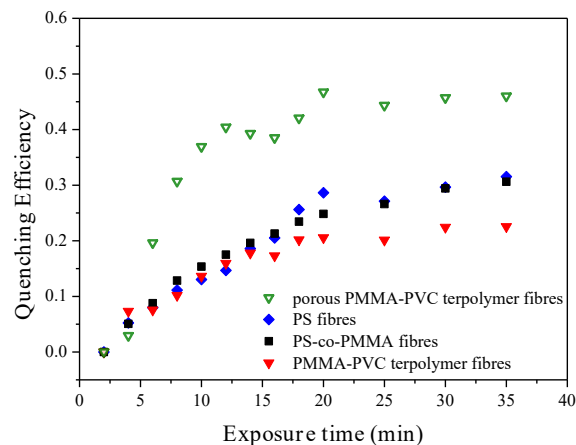


Fig. 7 Quenching efficiencies of pyrene-doped PS fibres, PS-co-PMMA fibres, PMMA-PVC terpolymer fibres, and porous PMMA-PVC terpolymer fibres as a function of exposure time to DNT vapour.

at 465 nm could be ascribed to the emission from excited pyrene excimers^{15,16}.

Upon exposure in saturated DNT vapour, fluorescence quenching of pyrene was observed due to electron transfer from excited pyrene to electron-deficient quencher, DNT^{3,17}. The electron transfer mechanism was provided in Fig. 6. As the mechanism is based on the electron-deficient DNT to accept the excited-state electron from pyrene, the main driving force is the energy gap between conduction band of pyrene and the lowest unoccupied molecular orbital of DNT³.

Pyrene-doped PS fibres, PS-co-PMMA fibres, and porous PMMA-PVC terpolymer fibres exhibited similar emission spectra to that of PMMA-PVC terpolymer fibres with two major bands. Emission intensity was found to decrease with increasing exposure time. The fluorescence quenching efficiencies of all prepared fibres as a function of exposure time were shown in Fig. 7. The time dependence of quenching was observed for all sensing fibres. The quenching reached a plateau after approximately 20 min. In addition, the sensing performance was slightly improved in the presence of PS. PS fibres and PS-co-PMMA fibres exhibited higher quenching efficiencies than PMMA-PVC terpolymer fibres, possibly due to the $\pi-\pi$ stacking between pyrene and the phenyl groups of PS^{3,6}. Although PS fibres was expected to provide higher sensing performance than PS-co-PMMA fibres due to a higher PS content, the performance was likely offset by the larger fibre size. A pronounced sensing enhance-

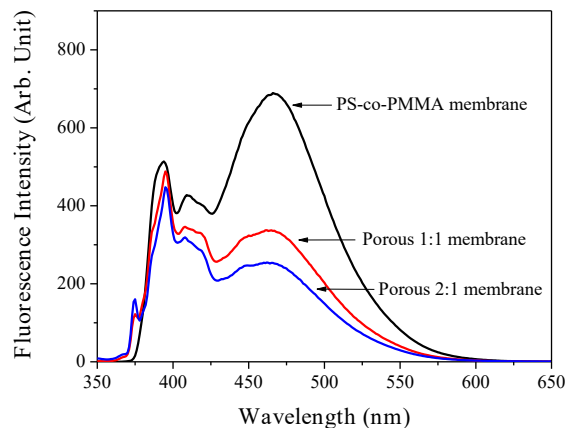


Fig. 8 Emission spectra of pyrene-doped PS-co-PMMA membrane and two porous PS-co-PMMA membranes ($\lambda_{\text{Ex}} = 336 \text{ nm}$).

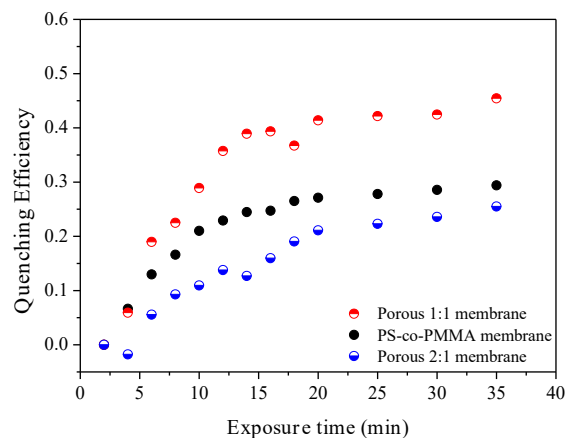


Fig. 9 Time-dependent quenching efficiencies of dense and porous PS-co-PMMA membranes.

ment was achieved through the introduction of secondary porous structures to PMMA-PVC terpolymer fibres. A maximum quenching efficiency of 0.46 was obtained. Noting that the effect of secondary porous structures on sensing performance was only investigated for PMMA-PVC terpolymer fibres due to relatively low mechanical strength of PS fibres and PS-co-PMMA fibres.

Membranes

The effect of porous structure on DNT sensing was further explored in membrane. PS-co-PMMA was chosen as polymer matrix due to the presence of PS groups and flexibility. Emission spectra of pyrene-

doped PS-co-PMMA membrane and two porous PS-co-PMMA membranes were shown in Fig. 8. The emission intensities of excited pyrene monomer between 370 and 420 nm increased in the presence of porous structures, suggesting a less aggregation of pyrene.

The fluorescence quenching efficiencies of all prepared membranes as a function of exposure time were shown in Fig. 9. Porous 1:1 membrane demonstrated the highest quenching efficiency, followed by dense PS-co-PMMA membrane, and porous 2:1 membrane. The enhanced efficiency of porous 1:1 membrane was attributed to the increased surface area. Although porous 2:1 membrane contained a larger number of pores, a reduced quenching efficiency might result from the leaching out of pyrene during PEG removal.

The role of material types, fibre versus membrane, on sensing performance towards DNT was not significantly observed. Even though, PS-co-PMMA fibres possessed much higher surface area than PS-co-PMMA membrane, a slightly higher performance was shown. This could be explained by the negative effect of the greater thickness of fibres (0.41 versus 0.25 mm), where pyrene located inside the fibre mat could not be quenched easily by DNT.

CONCLUSIONS

This work provides simple, efficient, and low cost approaches to fabricate fluorescence quenching-based optical sensors for DNT detection. The effect of electrospun polymer matrix on DNT sensing was observed. Pyrene-doped PS fibres and PS-co-PMMA fibres provided slightly higher quenching efficiencies than PMMA-PVC terpolymer fibres. Porous PMMA-PVC terpolymer/pyrene fibres from 30% PEG solution showed an enhanced quenching efficiency compared to nonporous fibres with the value of 0.46. In addition, PS-co-PMMA/pyrene membrane and two porous PS-co-PMMA/pyrene membranes with different pore numbers and sizes were prepared. A complete removal of PEG progen was obtained after 2 days of immersion in water as confirmed by FTIR and SEM. Porous 1:1 membrane displayed higher sensing performance towards DNT than dense PS-co-PMMA membrane. Among tested materials, porous PMMA-PVC terpolymer fibres and porous 1:1 PS-co-PMMA membrane demonstrated the highest quenching efficiencies of 0.4 after 20 min of exposure time, probably due to the higher surface areas.

Acknowledgements: This work has been partially supported by the Research Network NANOTEC (RNN) program of the National Nanotechnology Centre (NANOTEC), NSTDA, Ministry of Science and Technology and Khon Kaen University, Thailand, and the Centre for Innovation in Chemistry (PERCH-CIC), Office of the Higher Education Commission, Ministry of Education. The authors gratefully thank Chonnakarn Panawong and Kwanjira Panplado for instrumental help.

REFERENCES

1. Wang XY, Drew C, Lee SH, Senecal KJ, Kumar J, Sarnuelson LA (2002) Electrospun nanofibrous membranes for highly sensitive optical sensors. *Nano Letters* **2**, 1273–5.
2. Guo L, Zu B, Yang Z, Cao H, Zheng X, Dou X (2014) APTS and rGO co-functionalized pyrenated fluorescent nanonets for representative vapor phase nitroaromatic explosive detection. *Nanoscale* **6**, 1467–73.
3. Wang Y, La A, Ding Y, Liu Y, Lei Y (2012) Novel signal-amplifying fluorescent nanofibers for naked-eye-based ultrasensitive detection of buried explosives and explosive vapors. *Adv Funct Mater* **22**, 3547–55.
4. Yang YF, Wang HM, Su K, Long YY, Peng Z, Li N, Liu F (2011) A facile and sensitive fluorescent sensor using electrospun nanofibrous film for nitroaromatic explosive detection. *J Mater Chem* **21**, 11895–900.
5. Yang YF, Fan X, Long YY, Su K, Zou DC, Li N, Zhou J, Li K, et al (2009) A simple fabrication of electrospun nanofiber sensing materials based on fluorophore-doped polymer. *J Mater Chem* **19**, 7290–5.
6. Panawong C, Pandhumas T, Youngme S, Martwiset S (2015) Enhancing performance of optical sensor through the introduction of polystyrene and porous structures. *J Appl Polym Sci* **132**, 41759.
7. Pandhumas T, Panawong C, Loiha S, Martwiset S (2017) Porous electrospun fibers as optical sensor for metal ion. *Chiang Mai J Sci* **44**, 1704–13.
8. Tanford C (1961) *Physical Chemistry of Macromolecules*, John Wiley & Sons Inc., New York.
9. Eda G, Shivkumar S (2007) Bead-to-fiber transition in electrospun polystyrene. *J Appl Polym Sci* **106**, 475–87.
10. Ramesh S, Leen KH, Kumutha K, Arof AK (2007) FTIR studies of PVC/PMMA blend based polymer electrolytes. *Spectrochim Acta Mol Biomol Spectrosc* **66**, 1237–42.
11. Pizarro GC, Jeria-Orell M, Marambio OG, Olea AF, Valdés DT, Geckeler KE (2013) Synthesis of functional poly(styrene)-block-(methyl methacrylate/methacrylic acid) by homogeneous reverse atom transfer radical polymerization: Spherical nanoparticles, thermal behavior, self-aggregation, and morphological properties. *J Appl Polym Sci* **129**, 2076–85.
12. Zhang L, Li C, Liu A, Shi G (2012) Electrosynthesis of graphene oxide/polypyrene composite films and their applications for sensing organic vapors. *J Mater Chem* **22**, 8438–43.
13. Xue Y, Patel A, Sant V, Sant S (2015) PEGylated poly(ester amide) elastomers with tunable physico-chemical, mechanical and degradation properties. *Eur Polym J* **72**, 163–79.
14. Focsaneanu KS, Scaiano JC (2005) Potential analytical applications of differential fluorescence quenching: pyrene monomer and excimer emissions as sensors for electron deficient molecules. *Photochem Photobiol Sci* **4**, 817–21.
15. Shiraishi Y, Tokitoh Y, Hirai T (2006) pH- and H₂O-driven triple-mode pyrene fluorescence. *Org Lett* **8**, 3841–4.
16. Pietsch C, Hoogenboom R, Schubert US (2010) PMMA based soluble polymeric temperature sensors based on UCST transition and solvatochromic dyes. *Polymer Chemistry* **1**, 1005–8.
17. Bodenant B, Fages F, Delville MH (1998) Metal-induced self-assembly of a pyrene-tethered hydroxamate ligand for the generation of multichromophoric supramolecular systems. The pyrene excimer as switch for iron(III)-driven intramolecular fluorescence quenching. *J Am Chem Soc* **120**, 7511–9.